Ionic Conduction of Lithium Electrolyte Close to the Cathode Active Materials : LiCoO2 powder/ non-aqueous LiClO4 solution coexisting systems

Mizuhata, Minoru
Inagaki, Satoshi
Deki, Shigehito

(Citation)
ECS Transactions,2(27):31-40

(Issue Date)
2007

(Resource Type)
journal article

(Version)
Version of Record

(URL)
https://hdl.handle.net/20.500.14094/90005886

ECS Transactions, 2 (27) 31-40 (2007)
10.1149/1.2409025, copyright The Electrochemical Society

Ionic Conduction of Lithium Electrolyte Close to the Cathode Active Materials - $LiCoO_2$ powder/ non-aqueous $LiClO_4$ solution coexisting systems -

Minoru Mizuhata, Satoshi Inagaki, and Shigehito Deki

Department of Chemical Science and Engineering
Faculty of Engineering, Kobe University
1-1 Rokkodai-cho, Nada, Kobe 657-0036, JAPAN

The electrolyte conductivity was measured for the coexisting system containing the non-aqueous lithium electrolyte and lithium cobalt (III) oxide ($LiCoO_2$) powder utilized as the cathode active material. The anomalous behaviors of the ionic conduction near the solid surface were discussed. The conductivity increased with an increase of the liquid content and depended on the solvents. The values of each system depend on the order of the conductivity of bulk systems. Below 15 vol% of the liquid phase, the values were similar as each others. The activation energy was relatively low (20-25 kJ/mol) and decreased with the decrease of the liquid phase for the system containing $LiCoO_2$ powder, whereas the values increased for the system containing α-Al_2O_3 powder. The decrease phenomena of the activation energy were depends on the solvent species. The IR spectra showed the change of the solvation interaction between C=O bonding and Li^+ ion. It is suggested that the conductivity near the solid surface depends on the interaction between solid surface and the ionic species among the solvent molecules.

Introduction

Lithium cobalt(III) oxide, which has a rocksalt-type(HT) structure, is widely utilized for lithium-ion battery as the cathode active materials showing the smooth intercalation of lithium ions(1-2). Numerous studies have been carried out about the intercalation and transport phenomena of the ionic species and lithium cobalt oxide for the characterization during charge-discharge processes in the lithium-ion batteries (3, 4). In such systems, the transport phenomena of the ionic species are influenced by the change of solvation structure due to interaction between solid surface and the ionic species. In the other hand, various studies have been carried out for the properties of $LiCoO_2$, such as magnetic susceptibility (5), Raman spectroscopy in high pressure circumstance (6), reflectivity of millimeter wave for estimating discharge process (7), and so on. In these studies, the authors have focused the ionic transport in and around $LiCoO_2$ crystal as an intercalation compounds which depends on the direction of the ionic transportation and structural ordering for lithium secondary batteries. Therefore, the structure of $LiCoO_2$ was controlled and the conductivity was measured for single crystal (8), PLD thin films (9), and sputtered thin films (9, 10). $LiCoO_2$ was utilized for not only the lithium secondary batteries, also molten carbonate fuel cells (MCFCs), for electrode as an additives because of good conductive properties (11, 12). Such fundamental studies contributed to the knowledge accumulation of the materials. However the practical utilizations request to improve the performance as the energy devices and to combine with the useful additives to the active materials (13-16). In the viewpoints, composite materials containing $LiCoO_2$ have been developed and various kinds of properties such as charge-discharge performance (15), high-rate performance (16). Furthermore, the charge-discharge reaction on interface between electrolyte-electrode was discussed in several media (17, 18). Such studies insisted that the not only the contribution of the structure of $LiCoO_2$ also the structural change of the dissolved species and interface reaction on the surface of $LiCoO_2$ crystal. It seems that the structure and its properties of electrolyte solution close to the solid phase are important for the electrode reaction. However, transport properties in the non-aqueous electrolyte solution as a liquid phase have not been known well for the system coexisting with porous solid phase, such as metal oxide, fibrous polymer, and porous active materials.

We have been studied the conductive properties of the non-aqueous lithium electrolyte solution coexisting with various kinds of porous solid materials (19). The ionic transport in nano- and meso- pores contribute to the conductivity in porous media besides the improvement of the solvent holding more than 70 vol% of the volume fraction of the liquid phase. Also we measured the conductivity and ionic transport number of the non-aqueous lithium electrolyte solution coexisting cation-exchangeable clay minerals (20). The intercalated ionic species in the interlayer contribute to the conduction behavior. In this study, the electrolyte conductivity was measured for the coexisting system containing the non-aqueous lithium electrolyte and lithium cobaltate powder utilized as the cathode active material. The anomalous behaviors of the ionic conduction near the solid surface are discussed.

Experimental

Samples

Properties of lithium cobalt (III) oxide $LiCoO_2$ powder used in this study was shown in Table 1. Stoichiometric ratio of Li/Co are fixed chemically which confirmed by X-ray Fluorescence Spectrometer XRF-1800 (Shimadzu). Lithium oxide and cobalt (III) oxide are used as a reference samples. Prior to using for the conductivity measurement, $LiCoO_2$ powder was dehydrated at 400ºC for 4 hours in vacuo. The average diameter of the powder and its specific surface area are 200 μm and 1.41 m^2/g, respectively.

Several kinds of non-aqueous 1.0 mol/l $LiClO_4$ solution were used as the liquid phase. $LiClO_4$ powder was dried in vacuum furnace at 200ºC before dissolving into each solvent. Ethylene carbonate(EC), propylene carbonate(PC) and γ-butylolactone(GBL) were used as the solvents, which were dehydrated by molecular sieve 4A in glove box purged by Ar gas.

These solid powder and electrolyte solution were mixed thoroughly. The sample was molded into the tablet in the alumina press at 52 MPa for 30 minutes for electrical conductivity measurement. The liquid content, ϕ_l, of the sample are calculated as

Table 1. Properties of $LiCoO_2$ powder.

Average diameter	200 μm
Single crystallite size	10 μm
Specific surface area	1.41 m^2/g
Density	5.13 g/cm^3
pzc	5.4 in pH
Crystallite phase	rocksalt layered structure (HT)
Element ratio	Li/Co = 2

following equation:

$$\phi_l = (w_l/\rho_l) / (w_l/\rho_l + w_s/\rho_s) \qquad [1]$$

where w_l, w_s, ρ_l, and ρ_s are the weight of the liquid phase, the weight of the solid phase, the density of the liquid phase, and density of the solid phase, respectively. The value of ϕ_l ranged between 0.05-0.4, i.e. 5-40 vol% of the liquid phase.

The elution behavior of ionic species from the solid powder was confirmed by ICP measurement. After the each measurement, no change of the crystal structure of the solid phase was observed by XRD and XPS measurements.

Measurement of the Electrical Conductivity

The measuring sample was sandwiched by platinum plate electrode with the diameter of 10 mm. The AC impedance was measured in air-tight sample cell at 5Hz-30MHz using precision LCR meter HP4284A and HP4286A (Agilent technology). The conductivity was calculated from the lowest frequency point of continuous and flattened semicircular arcs in equivalent circuit estimated from Nyquest plots of the obtained impedance. Since temperature dependence of the conductivity was cleared by log σ vs $1/T$ plots, the activation energy was calculated using Arrhenius equation.

Measurement of Diffusive Reflectance FT-IR spectra

In order to discuss an intramolecular vibration which indicates an interaction between solvent molecular and ions, IR spectra was measured using FT-IR spectrophotometer FT-IR 615R (JASCO Instrument) coupled with a diffuse reflectance attachment DR-600B (JASCO Instrument). A MCT (mercury–cadmium–telluride) detector cooled by liquid nitrogen was used. The diffuse reflectance cell was connected to the heating and temperature control system equipped with a thermocouple. Prior to the measurements, each sample was sealed into air-tight cell to which incident light came through single crystal KBr window. Spectra were obtained as the ratio of the auto single-beam scans to the same number of background scans for pure KBr. The resolution was 4 cm^{-1}. The change of the solvation structure with the coexistence of the powder sample was discussed from the results of the IR spectra measurements. The analysis of the DR-FTIR has been carried out by the same procedure as described in Ref. 21 and 22.

Results and discussion

Confirmation of Stability and Conductivity of the $LiCoO_2$

Since $LiCoO_2$ powder has a rocksalt-type structure, the electronic conduction might be observed certainly for the original powder. However, the conductivity of the $LiCoO_2$ powder without mixing with the liquid phase are ranged at 10^{-7} Scm^{-1}, which is much less than ionic conduction measured for the coexisting systems. It is suggested that powder was randomly packed in the tablet samples and junction was not completely connected in this sample. Therefore, the ionic conduction was not observed without electrolyte solution in this system.

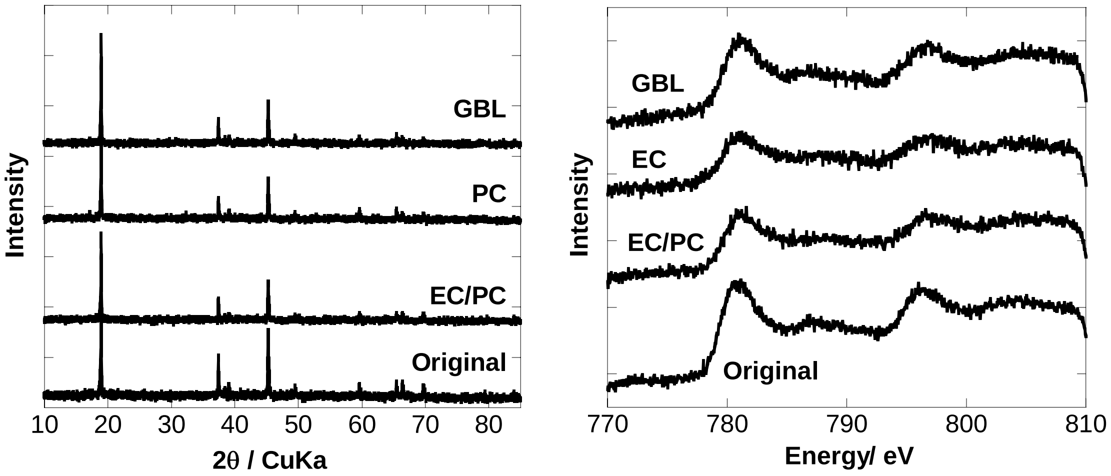

Figure 1. Variations of XRD patterns and XPS spectra with solvent species during measurements of conductivity for 7 days. For both cases, there are data for original $LiCoO_2$ powder.

Table 2. Elution amount of ionic species from $LiCoO_2$ powder (4g) after 7 days into various solvents of 40 mL (ppm).

Solvents	EC/PC(8:2)	PC	GBL
Li^+	17.3	10.2	44.5
Co^{n+}	21.9	10.9	15.6

Also, the composition stability of the samples was also confirmed during the measurement by ICP, XRD, and XPS. As shown in Figure 1, No change was observed for XRD and XPS spectra between original samples and used samples for every measurement procedures of conductivity and FT-IR. Then, the measured conductivity was caused form ionic conduction mainly, of which path was the lithium electrolyte solution penetrating among the $LiCoO_2$ powder.

AC Impedance and Electrical Conductivity

Typical obtained AC impedance is shown in Figure 2. The continuous loci were observed at the middle frequency range which shows the non-uniform relaxation in the system containing $LiCoO_2$ powder. The resistance of the sample is obtained from the lowest frequency of the continuous relaxation range. It means that the ionic transfer has a various time constants which cannot be separated in the proper frequency range. On thi other hand, the single relaxation range was observed in Figure 2b for the system containing α-Al_2O_3 powder which act as insulate matrix. It is suggested that $LiCoO_2$ can transfer the ionic species, which is estimated as Li^+ ion and of which mobility was depends on the conductive circumstance close to the surface properties of the solid phase such as ion-exchangeable matrixes (19, 20). Following impedance measurement, an electrical conductivity was calculated for each system. Variations of the electrical conductivity with the liquid content for the system containing 1.0 mol/l $LiClO_4$ electrolyte solution coexisting $LiCoO_2$ and α-Al_2O_3 powder.

The conductivity increased with an increase of the liquid content and depended on the solvents. The order of the conductivity at the same composition was GBL>EC>PC, which is the same one as that of the bulk solution (23). However, for the $LiCoO_2$ system, the values of an electrical conductivity were similar as each other below 15 vol% of the liquid phase, as shown in Figure 3a, whereas the difference among the solvent species are obviously observed for the system containing α-Al_2O_3 powder as shown in Figure 3b. It means that the ionic transporting circumstance becomes resemble in the systems using every solvent and does not depend on the solvent species for the system containing $LiCoO_2$ powder.

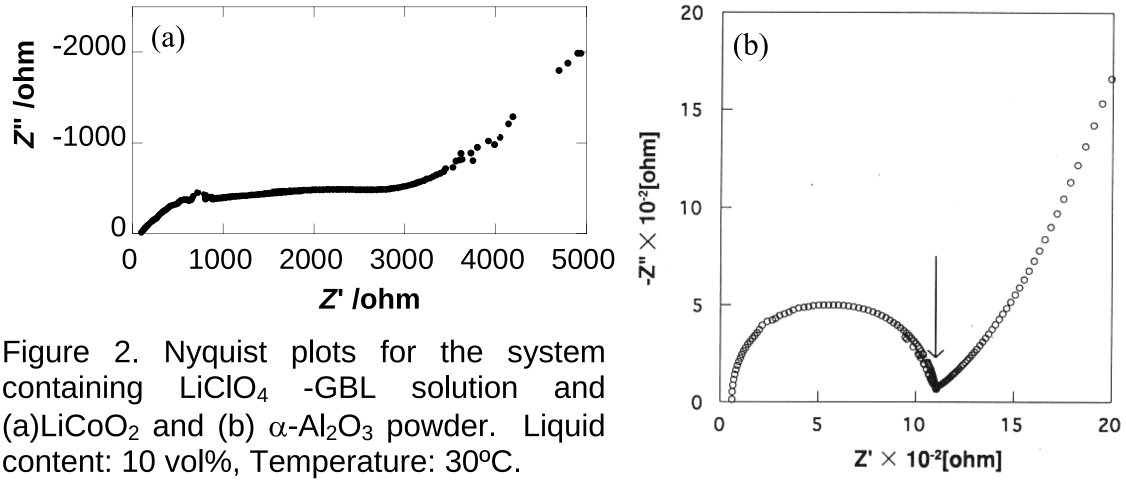

Figure 2. Nyquist plots for the system containing $LiClO_4$ -GBL solution and (a)$LiCoO_2$ and (b) α-Al_2O_3 powder. Liquid content: 10 vol%, Temperature: 30°C.

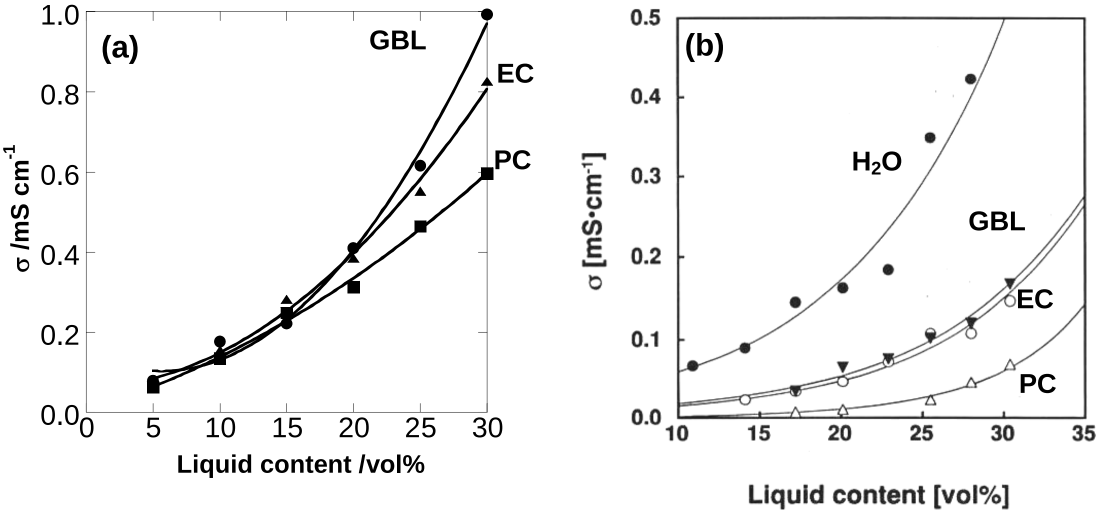

Figure 3. Variations of the electrical conductivity with the liquid content for the system containing 1.0 mol/l $LiClO_4$ electrolyte solution coexisting (a) $LiCoO_2$ and (b) α-Al_2O_3 powder. Temperature: 30°C.

Activation Energy of Electrical Conductivity

In order to discuss the ionic conductivity near the $LiCoO_2$ surface, the activation energy of the electrical conductivity for the system containing $LiCoO_2$ powder and $LiClO_4$ solution. The temperature dependence of the electrical conductivity on log σ vs. $1/T$ is shown in Figure 4. The plots bent from the linear relationship between log σ and $1/T$ which indicates Arrhenius one. In this case, we have applied the VTF equation which was introduced to conductivity by Adams and Angell et al. using free-volume theory (24-26) as follows.

$$\sigma = A\, T^{-1/2} \exp\left[-B/(T-T_0)\right] \quad [2]$$

In this case, the activation energy can be obtained from the differential coefficient led from Eq.[2] at each measuring temperature. The activation energy of the conductivity at 30ºC was shown in Figure 5 for the systems using each solvent. This parameter has been led in order to estimate the distance from the solid surface influenced to the structure and properties of the electrolyte solution near the solid phase (19, 27). Here, the activation energy depended on the apparent average thickness of the liquid phase on the solid surface. The activation energy was relatively low (20-25 kJ/mol) and decreased with the decrease of the liquid phase for the system containing

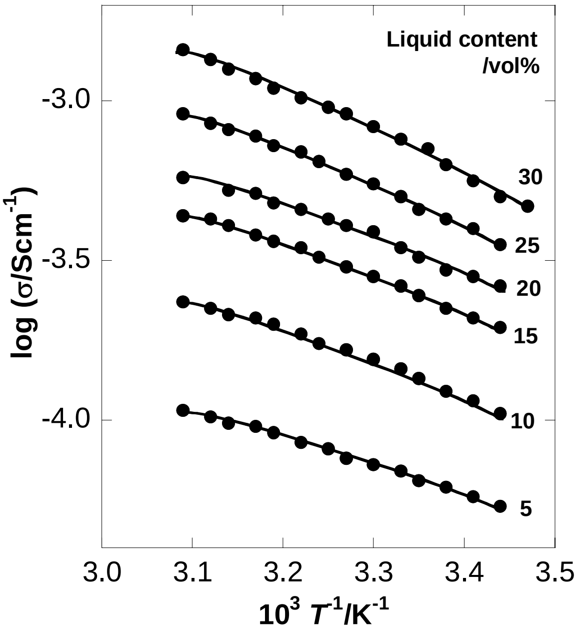

Figure 4. Temperature dependence of the electrical conductivity for the system containing $LiClO_4$–EC solution and $LiCoO_2$ powder.

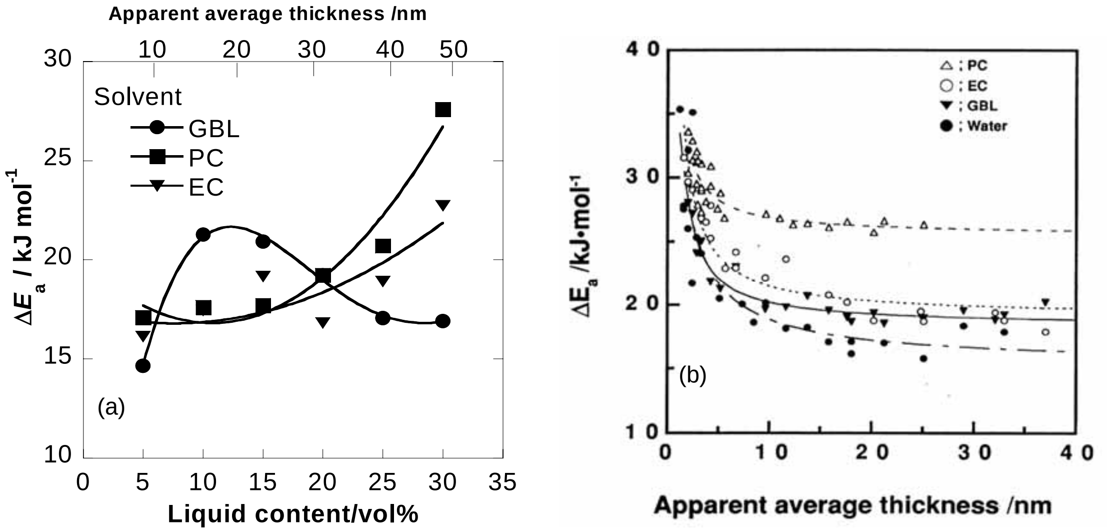

Figure 5. Variations of activation energy of the electrical conductivity for the system containing inorganic powder ((a) $LiCoO_2$, (b) α-Al_2O_3), and non-aqueous $LiClO_4$ solution. Temperature : 30°C.

$LiCoO_2$ powder, whereas the values increased for the system containing α-Al_2O_3 powder. The decrease phenomena of the activation energy were depends on the solvent species and as shown in Figure 5a. The tendency of the ionic transport was different between the systems containing $LiCoO_2$ and α-Al_2O_3 as the species of the solid phase. For $LiCoO_2$ system, the activation energy of the conductivity decreased with decreasing the apparent average thickness, whereas it increased with decreasing the thickness for the α-Al_2O_3 system. It is suggested that the Li^+ transport phenomena are influenced by the surface properties of $LiCoO_2$ powder and the solvation structure were weakened by the electrostatic interaction from the solid surface. Using $LiCoO_2$ powder, the Li^+ ion which interacts anion near the solid phase weakly, because of highly insertion rate through the surface, whereas α-Al_2O_3 powder does not have such effect.

The solvent effect was available to discuss the interaction between ion and solvent molecule for $LiCoO_2$ system. Using GBL which has a lower viscosity than EC or PC, the activation energy has maximum point near the solid surface of ca. 10 nm. Since PC and EC have highly ordered structure due to high dielectric constants causing a certain solvation structure, and the effect of the solid phase are relatively large competitively. Desolvated Li^+ ion can move easily stabilized by the solid surface, therefore the activation energy of the conductivity decreased as the liquid phase decreased.

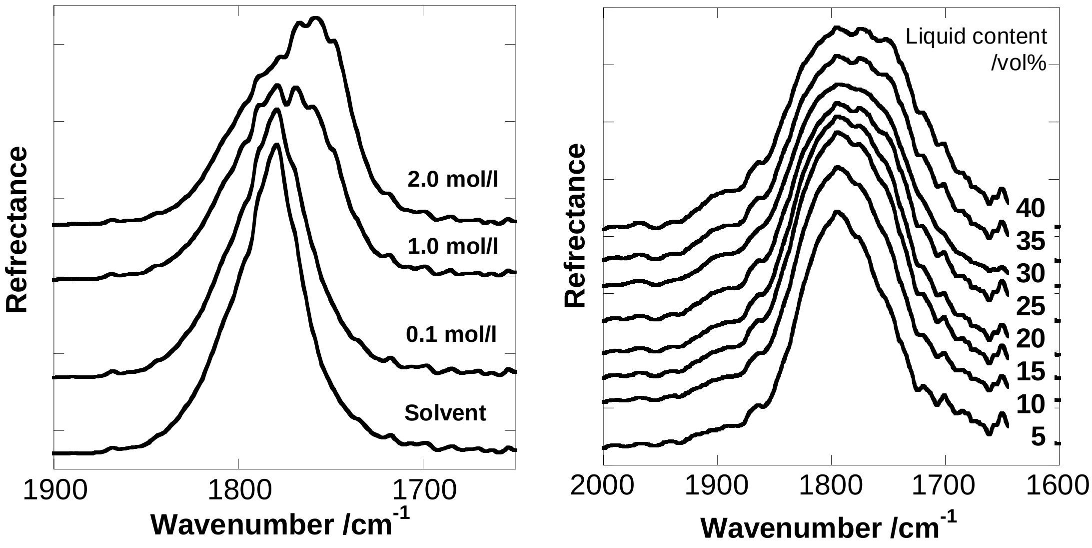

Figure 6. Diffuse reflectance FT-IR spectra for C=O stretching mode of propylene carbonate (PC) in (a) $LiClO_4$ –PC solution (bulk) and (b) coexisting system containing $LiClO_4$ –PC solution and $LiCoO_2$ powder of which liquid content ranges from 5 to 40 vol%.

FT-IR Spectroscopy and Interaction between Dissolving Species and Solid Surface

The IR spectra showed the change of the solvation interaction between solvent and Li ion. The stretching mode of C=O in propylene carbonate (PC) in $LiClO_4$-PC solution is shown in Figure 6. Promoting solvation between PC and Li^+ ion, Stretching mode of C=O shifted lower wavenumbers due to weakening intramolecular bonding by dipole-ion interaction; Li^+--O=C solvation interaction (27). However, coexisting with $LiCoO_2$ powder of which amount is 5-20 vol% of liquid phase, the band at lower wavenumbers was weakened and eliminated, as the liquid phase decreased. In such case, the organic moleculars are dissociate and interacted to the solid phase. Deconvoluting the C=O vibration mode, there are several vibration mode was found;

- Ring stretching + ring bending of PC at ca. 1800 cm^{-1}
- C=O stretching (free) at ca. 1780 cm^{-1}
- C=O stretching (solvated) at ca. 1760 cm^{-1}
- Ring stretching + C=O bending at ca 1740 cm^{-1}

It is suggested that the conductivity near the solid surface depends on the interaction between solid surface and the ionic species among the solvent molecules. The intensity ratio of

$$I_{\text{solvated}}/I_{\text{free}} = \frac{[\text{C=O stretching (free) at ca. 1780 cm}^{-1}]/}{[\text{C=O stretching (solvated) at ca. 1760 cm}^{-1}]} \qquad [3]$$

is indicated as the ionic solvation index of $LiClO_4$ –PC solution/ $LiCoO_2$ powder in Figure 7. In the bulk solution, the value of $I_{\text{solvated}}/I_{\text{free}}$ increased with concentration of the $LiClO_4$ solution due to the ion solvation. However, coexisting system, the ratio decreased and reach to less than 0.5. It is suggested that the interaction between Li and O=C are weakened, and Li^+ ion was desolvated from PC molecules. For each system, the intensity decreased because the desolvated PC was interacted to the surface of the solid

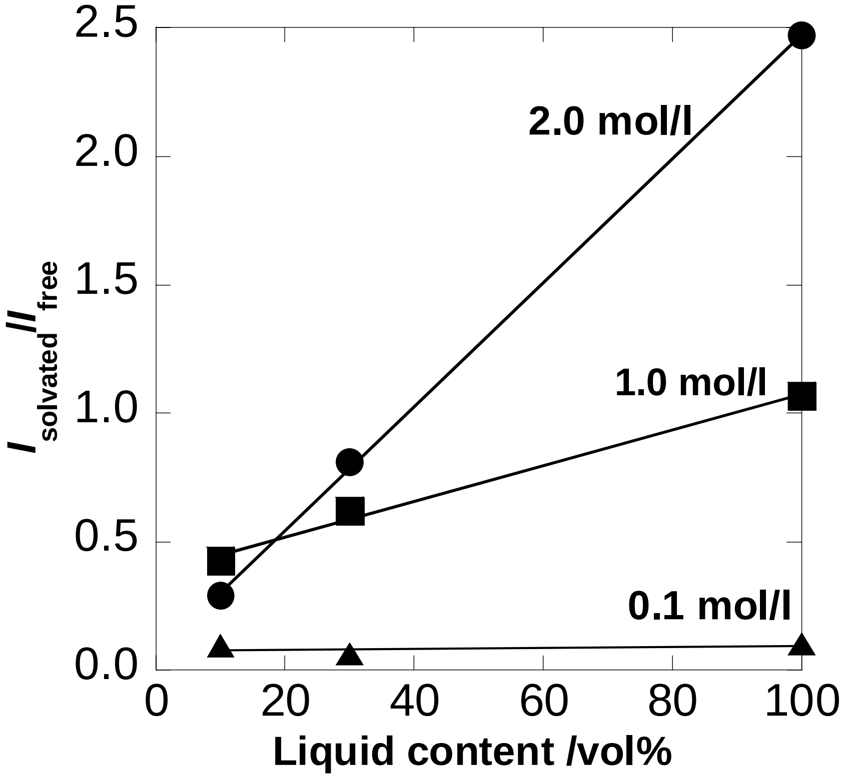

Figure 7. Intensity ratio; I_{solvated} / I_{free} of diffuse reflectance FT-IR of C=O stretching bonding for $LiClO_4$-PC solution coexisting with $LiCoO_2$ powder.

phase. In such case, the oriented PC molecule causes the decrease of the dielectric field near the solid surface and the ionic interaction might increase (28). At the same system, O-C-O in PC molecular stretching band was also observed in FT-IR spectra. The stretching band of O-C-O bonding shifted higher wavenumbers which is complementary to C=O stretching bands. It is suggested that the location of the Li solvation was changed by the interaction between solid phase and PC molecular, from C=O bonding to O in O-C-O bonding mainly.

Conclusions

The conductivity and diffuse reflectance FT-IR spectra was measured for the system containing non-aqueous $LiClO_4$ solution and $LiCoO_2$ powder.

The electrical conductivity decreased as the liquid content decreased. At the liquid content less than 15 vol%, the conductivity does not depend on the kinds of solvent, EC, PC, and GBL. It is suggested that the ionic conductivity on the solid surface are promoted on $LiCoO_2$. The solvation of Li interacting to O=C bond of PC molecules are weakened by the interaction between solid phase and PC molecules and the band shift of O=C stretching band decreased. Comparing with the results for α-Al_2O_3 powder / $LiClO_4$ solution coexisting system, the variation of the activation energy of the electrical conductivity decreased as the liquid content decreases. It is suggested that the transport of the ionic species are promoted near the $LiCoO_2$ surface even any solvents were used, since the solvation of Li^+ ion was weakened, the free ions are interacted to the solid phases. In the case of α-Al_2O_3 system, the resemble phenomena were observed, however, the activation energy increased with decreasing the apparent average thickness of the liquid phase.

These results show the structure of the ionic solvation in the non-aqueous solution changes close to the solid phase; i. e., in the liquid layer having several ten's nanometer from the solid surface, and ionic transport phenomena were influenced and depend on the ionic mobilities on and in the solid phase. The phenomena of the charge transfer might be influenced to such structural changes of the ionic species near the solid surface.

References

1) S. Levasseur, M. Menetrier, E. Suard, C. Delmas, *Solid State Ionics*, **128**, 11 (2000).
2) E. Antolini, *Solid State Ionics*, **170**, 159 (2004).
3) Y. Iriyama, M. Inaba, T. Abe, and Z. Ogumi, *J. Power Sources*, **94**, 175(2001).
4) Y. Iriyama, T. Kako, C. Yaba, T. Abe, and Z. Ogumi, *Solid State Ionics*, **176**, 2371 (2005).
5) D. G. Kellerman, V. R. Galakhov, A. S. Semenova, Y. N. Blinovskov, and O. N. Leonidova, *Phys. Solid State*, **48**, 548 (2006).
6) X. Wang, I. Loa, K. Kunc, K. Syassen, and M. Amboage, *Phys. Rev. B*, **72**, 224102 (2005).
7) H. Ishikawa, T. Hirano, Y. Nagasaka, K. Kawakami, H. Ohta, T. Nanba, A. Hirano, R. Kanno, *J. Phys. Chem. Solid*, **66**, 2065 (2005).
8) Y. Takahashi, Y. Gotoh, J. Akimoto, S. Mizuta, K. Tokiwa, and T. Watanabe, *J. Solid State Chem.*, **164**, 1 (2002).
9) P. J. Bouwman, B. A. Boukamp, H. J. M. Bouwmeester, and P. H. L. Notten, *J. Electrochem. Soc.*, **149**, A699 (2002).

10) K. J. Rao, H. Benqlilou-Moudden, G. Coutuirier, P. Vinatier, and A. Levasseur, *Mater. Res. Bull.*, 37, 1353 (2002).
11) A. Wijayasinghe, B. Bergman, and C. Lagergren, *Solid State Ionics*, **177**, 165 (2006).
12) A. Wijayasinghe, B. Bergman, and C. Lagergren, *Solid State Ionics*, **177**, 175 (2006).
13) L. J. Fu, H. Liu, C. Li, Y. P. Wu, E. Rahm, R. Holze, and H. Q. Wu, *Solid State Sci.*, **8**, 113 (2006).
14) R. Dominko, M. Gaberšček, J. Drofenik, M. Bele, and J. Jamnik, *Electrochim. Acta.*, **48**, 3709 (2003).
15) S. Oh, J. K. Lee, D. Byun, W. I. Cho, and B. W.Cho, *J. Power Sources*, **132**, 249 (2004).
16) S. Huang, Z. Wen, X. Yang, Z. Gu, and X. Xu, *J. Power Sources*, **148**, 72 (2005).
17) H. Sakaebe, H. Matsumoto, and K. Tatsumi, *J. Power Sources*, **146**, 693 (2005).
18) H-S. Kim, K-S. Kum, W-I. Cho, B-W Cho, H-W Rhee, *J. Power Sources*, **124**, 221 (2003).
19) M. Mizuhata, M. Kitamura, and S. Deki, Electrochemistry, **71**, 1093 (2003).
20) M. Mizuhata, F. Ito, S. Deki, *J. Power Sources*, **146**, 365 (2005).
21) A. B. Béléké, M. Mizuhata, A. Kajinami, and S. Deki, *J. Colloid and Interface Sci.*, **268**, 413 (2003).
22) A. B. Béléké, M. Mizuhata, and S. Deki, *Phys. Chem. Chem. Phys.*, **5**, 2089 (2003).
23) M. Mizuhata, G.-J. Cha, I. Shige, A. Kajinami, S. Deki, in *Advanced Batteries and Super Capacitors*: 2001, G.A. Nazri, E. Takeuchi, R. Koetz, B. Scrosati, Editors, PV2001-21, p. 549, The Electrochemical Society Proceedings Series, Pennington, NJ (2001).
24) G. Adam and J. H. Gibbs, *J. Chem. Phys.,* **31**, 1164 (1959).
25) C. A. Angell, *J. Phys. Chem.*, **68**, 218 (1964).
26) C. A. Angell, *J. Phys. Chem.*, **68**,1917 (1964).
27) H. L. Yeager, J. D. Fedyk, R. J. Parker, *J. Phys. Chem.*, **77**, 2407 (1973).
28) S. Deki, M. Mizuhata, S. Nakamura, K. Nakamura, A. Kajinami, and Y. Kanaji, **139**, 996 (1992).